Original Article

Comparison of the diagnostic performance of contrast-enhanced ultrasound and high-resolution magnetic resonance imaging in the evaluation of histologically defined vulnerable carotid plaque: a systematic review and meta-analysis

Chao Hou[1,2]^, Ji-Qing Xuan[1], Li Zhao[1], Ming-Xing Li[1], Wen He[2#], Hui Liu[1#]

[1]Department of Ultrasound, the Affiliated Hospital, Southwest Medical University, Luzhou, China; [2]Department of Ultrasound, Beijing Tiantan Hospital, Capital Medical University, Beijing, China

Contributions: (I) Conception and design: C Hou, W He, H Liu; (II) Administrative support: W He, H Liu; (III) Provision of study materials or patients: C Hou, JQ Xuan, L Zhao, MX Li; (IV) Collection and assembly of data: JQ Xuan, L Zhao; (V) Data analysis and interpretation: MX Li, W He; (VI) Manuscript writing: All authors; (VII) Final approval of manuscript: All authors.

[#]These authors contributed equally to this work as co-last authors.

Correspondence to: Hui Liu, MD. Department of Ultrasound, the Affiliated Hospital, Southwest Medical University, No. 25 Taiping Street, Jiangyang District, Luzhou 646000, China. Email: 190352889@qq.com; Wen He, MD. Department of Ultrasound, Beijing Tiantan Hospital, Capital Medical University, No. 119, South Forth Ring Road West, Fengtai District, Beijing 100070, China. Email: ttyyus_hewen@163.com.

Background: Vulnerable carotid plaque is closely associated with ischemic stroke. Contrast-enhanced ultrasound (CEUS) and high-resolution magnetic resonance imaging (HR-MRI) are two imaging modalities capable of assessing the vulnerability of carotid plaques. This systematic review aimed to compare the diagnostic performance of CEUS and HR-MRI in the evaluation of histologically defined vulnerable carotid plaques.

Methods: A systematic literature search with predefined search terms was performed on PubMed, the Cochrane library, Embase, and Web of Science from January 2001 to December 2023. Studies that evaluated the diagnostic accuracy of vulnerable carotid plaques confirmed by histology with CEUS and/or HR-MRI were included. The pooled values were calculated using a random-effects meta-analysis to determine diagnostic power.

Results: This analysis included a total of 839 patients from 20 studies comprising 1,357 HR-MRI plaques and CEUS 504 plaques. With the reference to histological results, all nine CEUS studies focused on the detection of intraplaque neovascularization (IPN), and three studies also examined morphological changes or ulcerated plaques; meanwhile, among the HR-MRI studies, seven predominantly focused on identifying intraplaque hemorrhage (IPH) and three mainly examined lipid-rich necrotic cores (LRNCs). The pooled sensitivity, specificity, positive likelihood ratio, negative likelihood ratio, diagnostic odds ratio, and the area under the curve (AUC) for CEUS studies were 0.85 [95% confidence interval (CI): 0.81–0.89], 0.76 (95% CI: 0.69–0.83), 3.41 (95% CI: 1.68–6.94), 0.14 (95% CI: 0.05–0.38), 27.68 (95% CI: 5.78–132.62), and 0.89 [standard error (SE) 0.06], respectively; for HR-MRI, these values were 0.88 (95% CI: 0.85–0.90), 0.89 (95% CI: 0.86–0.92), 7.49 (95% CI: 3.28–17.09), 0.17 (95% CI: 0.12–0.24), 49.13 (95% CI: 23.87–101.11), and 0.94 (SE 0.01), respectively. The difference in AUC between the two modalities was not statistically significant (Z=0.82; P=0.68).

^ ORCID: 0000-0003-1234-8744.

Conclusions: CEUS and HR-MRI are valuable noninvasive diagnostic tools for identifying histologically confirmed vulnerable carotid plaques and demonstrate similar diagnostic performance. CEUS is more capable of detecting IPN and morphological changes, while HR-MRI is more suited to classifying IPH and LRNCs.

Keywords: Ultrasonography; microbubble; magnetic resonance imaging (MRI); carotid artery; plaque

Submitted Mar 17, 2024. Accepted for publication Jul 05, 2024. Published online Jul 26, 2024.
doi: 10.21037/qims-24-540
View this article at: https://dx.doi.org/10.21037/qims-24-540

Introduction

Stroke as a significant threat to the health of individuals worldwide, ranks as the second leading cause of death globally, following ischemic heart disease (1). Ischemic stroke, which constitutes 62.4% of all stroke cases (2), is imposing a growing burden on young adults in regions with low scores sociodemographic indices such as North Africa, the Middle East, and Southeast Asia (3). Carotid atherosclerosis is recognized as a contributing factor to ischemic stroke, and the risk of stroke caused by carotid artery stenosis increases with advancing age (4). Specifically, vulnerable plaques, characterized by thin or ruptured fibrous caps, intraplaque neovascularization (IPN), intraplaque hemorrhage (IPH), lipid-rich necrotic cores (LRNCs), ulceration, or inflammation, are associated with an increased risk of distal cerebral artery emboli blockage (5), which can lead to ischemic stroke. Both IPN and IPH have been identified as independent predictors of stroke recurrence in ischemic stroke survivors (6,7). Therefore, the early detection and treatment of vulnerable plaques could prove to be an effective strategy in preventing both the initial occurrence and subsequent recurrence of stroke.

Contrast-enhanced ultrasound (CEUS) and high-resolution magnetic resonance imaging (HR-MRI) are two commonly used tools to assess plaque vulnerability. CEUS has high sensitivity and specificity in identifying IPN and ulceration and in outlining luminal morphology (8,9). Meanwhile, HR-MRI is capable of detecting IPH and LRNCs (10). However, despite their respective strengths, CEUS and HR-MRI are also associated with distinct disadvantages. For instance, HR-MRI provides high soft-tissue and spatial resolution but is limited by its high cost, lengthy examination time, tendency to induce claustrophobia, and susceptibility to potential interference from metal objects in the body. As it pertains to CEUS, in which the contrast agent can be eliminated through respiration with minimal anaphylactoid reactions, its resolution may be affected by pseudoenhancement, obesity, postural restrictions, and subcutaneous gas. Therefore, it is necessary to determine whether these two modalities can be used complementarily to identify vulnerable plaques, which can significantly impact clinical and personal intervention.

Although several meta-analyses have assessed the diagnostic performance of HR-MRI and CEUS individually and have demonstrated their efficacy in identifying vulnerable plaques (11,12), only one study has directly compared these modalities' ability to detect unstable plaques (13). This meta-analysis, conducted by Li *et al.* (13), was based on a limited sample size of nine original studies published as of December 2021 and thus does not completely represent the entire body of research in this field. Plaque ulceration is one feature of susceptible plaque, but Li *et al.* did not include histologically proven ulcerated plaques in their analysis. Furthermore, they did not investigate the differences in the specific components of plaques which the two imaging tools focus on for detection. Therefore, this study aimed to systematically compare the diagnostic accuracy of CEUS and HR-MRI in evaluating carotid plaque vulnerability as defined by histology via a meta-analysis and to determine whether CEUS can serve as an alternative modality to HR-MRI for plaque vulnerability assessment. We present this article in accordance with the PRISMA-DTA reporting checklist (14) (available at https://qims.amegroups.com/article/view/10.21037/qims-24-540/rc).

Methods

Data sources and search strategy

We systematically searched PubMed, the Cochrane library, Embase, and Web of Science for articles published in the English or Chinese language with an English-language abstract from January 2001 to December 2023. The

search strategy is shown in Table S1. The protocol of this systematic review has been registered in PROSPERO (International Prospective Register of Systematic Reviews; registration No. CRD42023494214).

Inclusion and exclusion criteria

We aimed to include all original studies that reported the diagnostic performance of CEUS and HR-MRI in the evaluation of carotid plaques. Two reviewers (J.Q.X. and L.Z.) independently assessed the titles and abstracts of the articles we searched. The inclusion criteria by category were as follows: (I) participants—patients with carotid plaque; (II) intervention and control—CEUS and/or HR-MRI examinations; (III) outcomes—diagnostic accuracy for identifying vulnerable plaques; (IV) study design—both observational (retrospective or prospective) and clinical trials; and (V) reference standard—histologically defined vulnerable plaques with one of the conditions of IPH, IPN, LRNC, thin or ruptured fibrous cap, ulceration, or inflammatory infiltrate being present. Meanwhile, the exclusion criteria were as follows: (I) duplicate patients or data; (II) animal studies; (III) insufficient information to create a 2×2 diagnostic table; (IV) case reports, narrative reviews, letters, editorial comments, and conference abstracts; and (V) a focus on cerebral vascular events caused by other diseases such as carotid dissection, vasculitis, or atrial fibrillation.

Data extraction and quality assessment

The variables extracted include the name of the first author; publication year; country; number of patients; gender; age; prevalence of diabetes, hypertension, smoking, dyslipidemia, and cardiovascular disease; study design; focused plaque composition based on histological results; patient type; and the technical details of CEUS and HR-MRI. To assess the risk of bias in the literature, we searched for the Journal Citation Reports (JCR) of journals in the year of publication of each study. We extracted or calculated the absolute number of true positives (TPs), false positives (FPs), false negatives (FNs), and true negatives (TNs) from each study even when multiple data sets were present. Two independent investigators (M.X.L. and W.H.) assessed the risk of bias and applicability concerns using the Quality Assessment of Diagnostic Accuracy Studies 2 (QUADAS-2) tool (15). Any disagreements were resolved by consensus.

Statistical analysis

This analysis was conducted using Meta-Disc version 1.4 (Ramón y Cajal Hospital, Madrid, Spain). Two-by-two tables were constructed for each study to calculate the sensitivity, specificity, positive likelihood ratio (LR+), negative likelihood ratio (LR–), diagnostic odds ratio (DOR), and their respective 95% confidence intervals (CIs). Moses linear models were used to generate a summary receiver operating characteristic (SROC) curve and calculate the area under the curve (AUC).

A Spearman correlation index between the logarithm of sensitivity and the logarithm of 1-specificity was applied to determine the presence of a threshold effect. A correlation coefficient greater than a certain value and a significance level of $P<0.05$ were indicative of a threshold effect; otherwise, a threshold effect was considered to be absent. Heterogeneity was assessed using either the chi-square test or Cochrane Q test. The I^2 statistic was employed to estimate the percentage of variability in results among studies that could be attributed to true differences in patients, tests, outcomes, and design rather than random chance. Values of 25%, 50%, and 75% were considered to represent low, moderate, and high inconsistency, respectively (16). The meta-analysis was carried out using a random-effects model in cases of moderate or high heterogeneity; otherwise, a fixed-effects model was used.

Subgroup analysis and sensitivity analysis were conducted to investigate the sources of heterogeneity. Subgroups were categorized by country, study design, sample sizes, plaque components, mechanical indexes (MIs), magnetic field strength, and journal JCR region. Sensitivity analysis involved the systematic one-by-one removal of studies. Deeks funnel plot of CEUS and MRI was generated using Stata version 17.0 (StataCorp, College Station, TX, USA) to assess publication bias. An asymmetry curve with $P\geq0.05$ indicated a lack of significant publication bias. The risk of bias and applicability were assessed using RevMan version 5.3 (Informatics and Knowledge Management Department, Cochrane, London, UK).

Results

Literature search

The systematic research retrieved 2,652 studies, 1,700 of which were found to be duplicated. Following the retrieval and evaluation of titles and abstracts, 850 studies

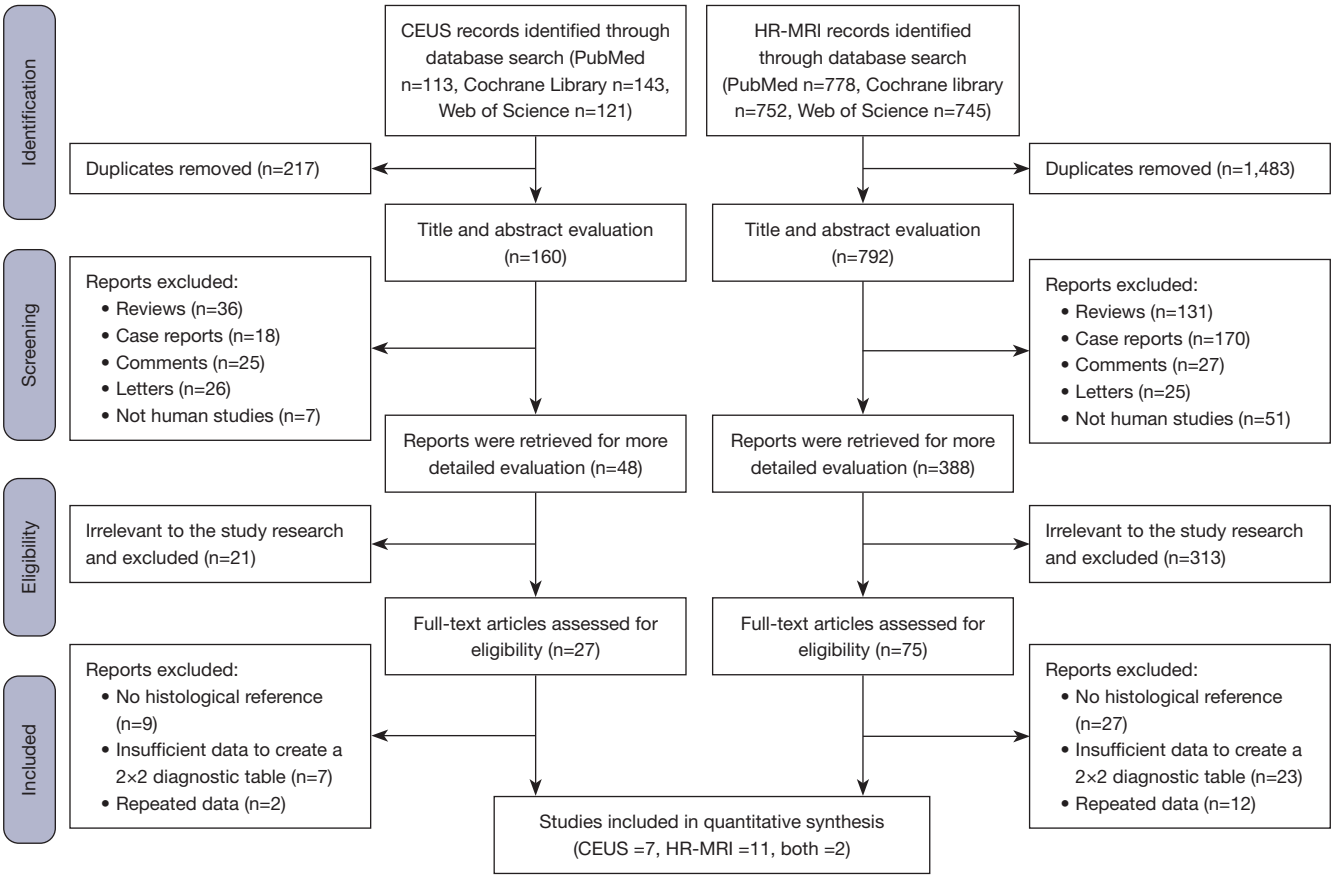

Figure 1 Flowchart of study selection using the PRISMA guidelines. CEUS, contrast-enhanced ultrasound; HR-MRI, high-resolution magnetic resonance imaging; PRISMA, Preferred Reporting Items for Systematic Review and Meta-Analysis.

were excluded. Subsequently, 102 studies were deemed eligible and for full-text review, with 20 ultimately meeting the inclusion criteria for this meta-analysis. Specifically, 7 studies focused on CEUS (17-23), 11 on HR-MRI (10,24-33), and 2 studies covered both modalities (34,35). A flowchart illustrating the research and selection process is presented in *Figure 1*.

Table 1 summarizes the clinical details of the 20 articles. A total of 839 patients were included; 3 studies did not report the gender components (17,21,29) or age distribution (17,29,30), respectively; and the remaining study population was composed 78.7% (528/671) of men and had a mean age of 70.15±4.24 years (n=687). The majority of studies were from China (30%), followed by Italy (25%), Japan (15%), and the United States (10%), while Switzerland, the United Kingdom, the Netherlands, and Germany each accounted for only 5% of the included literature. The population size varied from 11 to 101. Twelve studies (10,17,19,20,23,24,26-30,32) were published in JCR region 1 journals and six in JCR region 2 journals (18,22,25,31,33,34). The values of TPs, FPs, FNs, and TNs are available in *Table 1*.

Risk of bias and applicability

The results and details of the QUADAS-2 assessment for the 20 studies are summarized in *Figure 2A,2B* and Table S2. Although the overall quality of the 19 studies was moderate, the QUADAS-2 tool identified some potential sources of bias. Flow and timing emerged as the primary source of bias, followed by patient selection. In the flow and timing domain, the interval between the index test and reference test was unclear in 60.0% of the studies (19-22,24,25,27,28,31,33,35,36), and 20.0% of studies did not include all patients in the final analysis (23,29,31,33). Concerning the patient selection domain, 60.0% of studies

Table 1 The clinical characteristics of the included studies

First author (year)	Country	Age (years, mean ± SD)	Population size (men, %)	Patient type	TP (n)	FP (n)	FN (n)	TN (n)	DM (n)	HPN (n)	Smoking (n)	Dyslipidemia (n)	Symptomatic (n)	JCR region
Fresilli D (2022) (17)	Italy	NA	101 (NA)	Symptomatic stenosis ≥50% and asymptomatic stenosis ≥60%	64	1	7	29	NA	NA	NA	NA	NA	1
Huang S (2021) (18)	China	68.3±9.5	38 (34, 89.5%)	Carotid stenosis ≥50%	25	2	3	8	15	26	37	38	37	2
D'Oria (2018) (19)	Italy	72.8±6.6	58 (33, 56.9%)	Asymptomatic stenosis ≥70%	12	10	27	9	46	24	27	45	0	1
Lyu Q (2021) (20)	China	67±6.5	51 (43, 84.3%)	Symptomatic stenosis ≥50% and asymptomatic stenosis ≥70%	21	2	3	25	28	31	NA	NA	42	1
Di Leo (2018) (21)	Italy	69.8±8.5	43 (NA)	CEA	27	5	4	7	NA	NA	NA	NA	NA	NA
Iezzi R (2015) (22)	Italy	69.9±7.3	50 (28, 56.0%)	Carotid stenosis ≥70%	35	5	2	11	NA	NA	NA	NA	18	2
Uchihara Y (2023) (23)	Japan	71.7±1.05	68 (67, 98.5%)	CEA	61	1	1	5	21	58	12	50	47	1
Chai JT (2017) (10)	China	67.5	26 (19, 73.1%)	50–90% carotid stenosis	17	1	0	8	8	23	11	19	15	1
Hideki O (2010) (24)	United States	67.7±10.8	20 (16, 80.0%)	Carotid stenosis >80% and symptomatic stenosis >70%	40	4	10	130	5	14	11	16	NA	1
Narumi S (2015) (25)	Japan	70.4	34 (31, 91.2%)	Substantial stenosis	20	0	0	14	NA	NA	NA	NA	26	2
Puppini G (2006) (26)	Italy	72.5	19 (13, 68.4%)	Symptomatic carotid stenosis ≥70%	45	0	3	8	NA	NA	NA	NA	19	1
Moody AR (2003) (27)	United Kingdom	69	63 (33, 52.4%)	Carotid stenosis >70%	37	3	7	16	NA	NA	NA	NA	63	1
Cai JM (2002) (28)	China	70	60 (54, 90.0%)	CEA	75	14	17	146	NA	NA	NA	NA	NA	1
Kampschulte A (2004) (29)	Germany	NA	24 (NA)	CEA	134	9	6	41	NA	NA	NA	NA	NA	1
Chu B (2004) (30)	United States	NA	27 (21, 77.8%)	CEA	130	11	15	33	NA	NA	NA	NA	13	1
Qiao Y (2011) (31)	China	72	15 (13, 86.7%)	Carotid stenosis ≥58%	55	1	8	80	NA	NA	NA	NA	8	2

Table 1 (*continued*)

Table 1 (*continued*)

First author (year)	Country	Age (years, mean ± SD)	Population size (men, %)	Patient type	TP (n)	FP (n)	FN (n)	TN (n)	DM (n)	HPN (n)	Smoking (n)	Dyslipidemia (n)	Symptomatic (n)	JCR region
Cappendijk VC (2004) (32)	The Netherlands	68±4	11 (7, 63.6%)	Symptomatic carotid stenosis ≥70%	35	4	8	47	NA	NA	NA	NA	11	1
Tapis P (2020) (33)	Switzerland	71.5±8.68	36 (29, 80.6%)	Carotid stenosis ≥70%	19	0	13	4	6	23	12	28	25	2
Motoyama R (2019) (34)	Japan	71.5±6.5	70 (68, 97.1%)	Carotid plaque	44[a]/43[b]	8[a]/16[b]	4[a]/5[b]	14[a]/6[b]	21	60	12	52	48	2
Zhao KQ (2018) (35)	China	66.5	25 CEUS (19, 76%), 19 HR-MRI (19, 100%)	Symptomatic stenosis ≥50% and asymptomatic stenosis ≥70%	15[a]/10[b]	2[a]/2[b]	1[a]/2[b]	7[a]/5[b]	18	20	NA	NA	NA	NA

[a] value for contrast-enhanced ultrasound study; [b] value for high-resolution magnetic resonance imaging study. SD, standard deviation; TP, true positive; FP, false positive; FN, false negative; TN, true negative; DM, diabetes mellitus; HPN, hypertension; JCR, Journal Citation Reports; NA, not available; CEA, carotid endarterectomy; CEUS, contrast-enhanced ultrasound; HR-MRI, high-resolution magnetic resonance imaging.

did not clearly describe the inclusion and exclusion criteria (10,19,21,25-27,29-34), and participant enrollment was unclear in nine studies (10,18,19,26,29,30,32,33,35). Additionally, four studies (18,21,26,35) did not report whether the assessment was blinded or not, and three studies employed single blinding (17,22,25).

Synthesis of results

Threshold effects

The Spearman correlation coefficient of CEUS was –0.350 (P=0.356), while that of HR-MRI was 0.121 (P=0.694), indicating no threshold effects in the two diagnostic tests. The Cochran Q, I^2, and P values of the DOR for CEUS were 56.41, 85.8%, and <0.001, while those for HR-MRI were 34.19, 64.9%, and <0.001, respectively, representing high and moderate heterogeneity among the CEUS and HR-MRI studies, respectively. Therefore, a random-effects model was applied for the corresponding meta-analysis.

Diagnostic performances of CEUS and HR-MRI

All 20 studies used histology as the reference standard, and details of the methodology of each study are provided in *Table 2*. According to the histological findings, all CEUS studies focused on the detection of IPN, while three studies (17,18,20) also examined morphological changes or ulcerated plaques. The pooled sensitivity, specificity, LR+, LR–, DOR, and AUC were 0.85 (95% CI: 0.81–0.89), 0.76 (95% CI: 0.69–0.83), 3.41 (95% CI: 1.68–6.94), 0.14 (95% CI: 0.05–0.38), 27.68 (95% CI: 5.78–132.62), and 0.89 [standard error (SE) 0.06], respectively. In terms of HR–MRI, seven studies focused on identifying IPH (24,25,29-32,34), three studies on LRNC (10,26,33), and the remaining studies on complex components (27,28,35) (*Table 2*). The pooled sensitivity, specificity, LR+, LR–, DOR, and AUC were 0.88 (95% CI: 0.85–0.90), 0.89 (95% CI: 0.86–0.92), 7.49 (95% CI: 3.28–17.09), 0.17 (95% CI: 0.12–0.24), 49.13 (95% CI: 23.87–101.11), and 0.94 (SE 0.01), respectively (*Figures 3*,*4*). A Z test indicated that the pooled AUC differences between CEUS and HR-MRI were not statistically significant (Z=0.82; P=0.68).

Subgroup analysis

Subgroup analyses were employed to investigate the sources of heterogeneity for CEUS and HR-MRI in terms of DOR. A statistically significant level of P<0.05 indicated a possible source of heterogeneity. The findings suggested that factors

Figure 2 Risk of bias and applicability concerns of (A) each included study and (B) the overall judgment assessed using the revised Quality Assessment of Diagnostic Accuracy Studies 2.

including country, sample size, plaque component, and JCR region may contribute to the observed variability in CEUS and HR-MRI. In addition, the heterogeneity was also influenced by the MI in CEUS and magnetic field strength in MRI (*Table 3*, Tables S3,S4).

Sensitivity analysis

The results of the sensitivity analysis indicated that D'Oria *et al.*'s study (19) may be the primary cause of heterogeneity among the included CEUS studies. After this study was excluded, a fixed-effects model was used to assess the

Table 2 Summary of the methodological difference in studies

First author (year)	Research type	Plaque component confirmed by	CEUS				HR-MRI		
			Machine/probe	MI	Contrast agent	Analysis method	Device manufacture	Magnetic field strength	Sequence
Fresilli D (2022) (17)	R	IPN and ulceration	Samsung, RS80 and 85 Prestige, L3–L12	0.06–0.08	SonoVue	Qualitative G1–3	–	–	–
Huang S (2021) (18)	R	IPN and ulceration	Supersonic AixPlorer, 10–2L	NA	SonoVue	Qualitative G1–4	–	–	–
D'Oria (2018) (19)	P	IPN	MyLab, Esaote, 9L4	0.13	SonoVue	Quantitative/qualitative G0–3	–	–	–
Lyu Q (2021) (20)	P	IPN and morphology	Phillips iU-Elite, L9–3	<0.1	SonoVue	Qualitative G1–3	–	–	–
Di Leo (2018) (21)	R	IPN	Toshiba Aplio 500	0.05–0.07	SonoVue	Quantitative/qualitative G1–3	–	–	–
Iezzi R (2015) (22)	P	IPN	MyLab, Esaote	0.13	SonoVue	Qualitative G1–3	–	–	–
Uchihara Y (2023) (23)	R	IPN	GE LOGIQ E9	0.2–0.3	Sonazoid	Qualitative G0–3	–	–	–
Chai JT (2017) (10)	P	LRNC	–	–	–	–	Siemens	3.0 T	TOF, 2D T2 mapping
Hideki O (2010) (24)	P	IPH	–	–	–	–	Philips/GE	3.0 T	3D MPRAGE, 3D TOF, 2D T1FSE
Narumi S (2015) (25)	P	IPH	–	–	–	–	GE	1.5 T	3D-FSE T1WI and 2D spin-echo T1WI
Puppini G (2006) (26)	R	LRNC	–	–	–	–	Siemens	1.5 T	3D TOF, T1WI, T2WI, PDWI
Moody AR (2003) (27)	P	Complex	–	–	–	–	Siemens	1.5 T	MRDTI
Cai JM (2002) (28)	P	IPH, LRNC	–	–	–	–	GE	1.5 T	TOF, T1WI, T2WI, PDWI
Kampschulte A (2004) (29)	P	IPH	–	–	–	–	GE	1.5 T	TOF, T1WI, T2WI, PDWI
Chu B (2004) (30)	P	IPH	–	–	–	–	GE	1.5 T	3D TOF MRA, T1WI, T2WI, PDWI
Qiao Y (2011) (31)	R	IPH	–	–	–	–	Philips	3.0 T	3D FFE, 3D-TOF MRA
Cappendijk VC (2004) (32)	R	IPH	–	–	–	–	Philips	1.5 T	T1W TFE, T1W TSE
Tapis P (2020) (33)	R	LRNC	–	–	–	–	Siemens	3.0 T	3D TOF, T1WI, T2WI
Motoyama R (2019) (34)	P	IPN/IPH	GE LOGIQ E9, 9L	0.2–0.3	Sonazoid	Qualitative G0–G3	Siemens	3.0 T	MPRAGE
Zhao KQ (2018) (35)	P	IPN/complex	Toshiba Aplio i500, 11L	NA	NA	Qualitative G1–2	NA	NA	T1WI, T2WI, 3D TOF

CEUS, contrast-enhanced ultrasound; MI, mechanical index; HR-MRI, high-resolution magnetic resonance imaging; R, retrospective; IPN, intraplaque neovascularization; G, grade; NA, not available; P, prospective; LRNC, lipid-rich necrotic core; TOF, time of flight; 2D, two-dimensional; IPH, intraplaque hemorrhage; 3D, three-dimensional; MPRAGE, magnetization-prepared rapid acquisition with gradient echo; FSE, fast spin echo; T1WI, T1-weighted imaging; T2WI, T2-weighted imaging; PDWI, proton density-weight imaging; MRDTI, magnetic resonance direct thrombus imaging; MRA, magnetic resonance angiography; FFE, fast-field echo; TFE, turbo field echo; TSE, turbo spin echo.

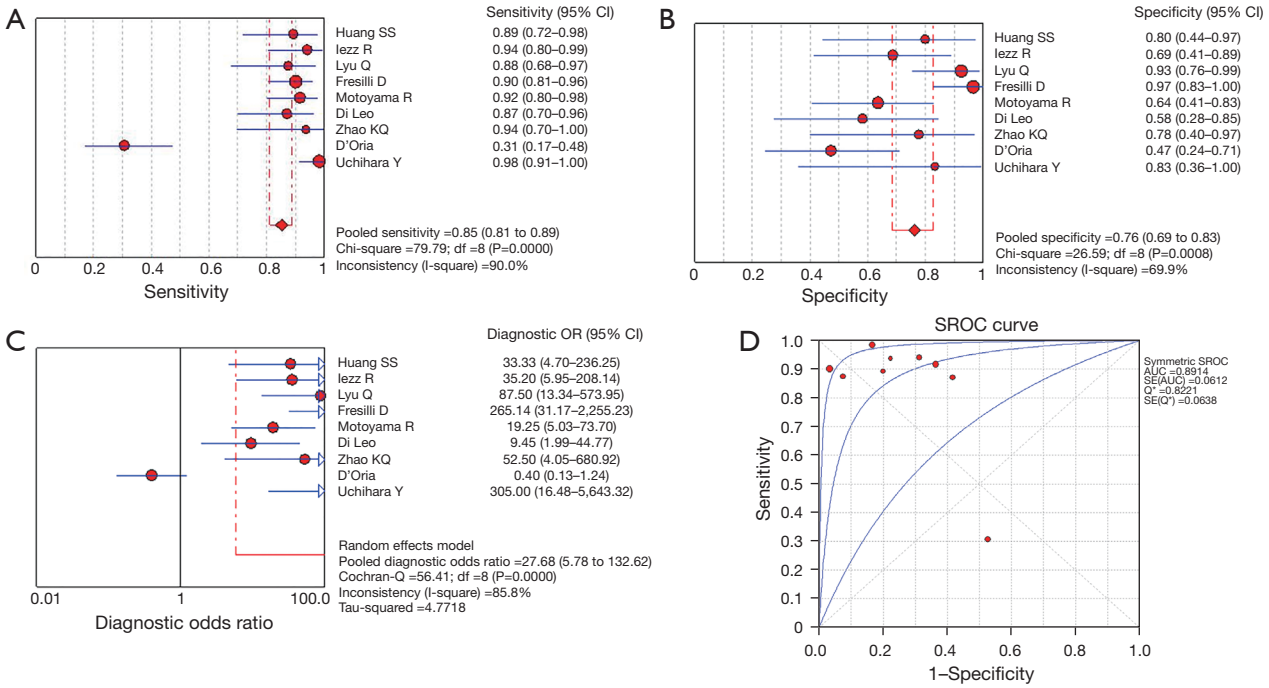

Figure 3 Forest plots of (A) sensitivity, (B) specificity, (C) diagnostic odds ratio, and (D) the summary receiver operator characteristic curve of the CEUS studies. In (D), the first and the third blue lines represent the 95% CI of AUC, and the second blue line represents the regression line. OR, odds ratio; CI, confidence interval; SROC, summary receiver operating characteristic; AUC, area under the curve; SE, standard error; CEUS, contrast-enhanced ultrasound.

combined values of the remaining CEUS studies. The pooled sensitivity, specificity, LR+, LR–, DOR, and AUC were 0.92 (95% CI: 0.88–0.95), 0.80 (95% CI: 0.72–0.87), 4.00 (95% CI: 2.35–6.81), 0.12 (95% CI: 0.08–0.17), 41.49 (95% CI: 18.47–93.23), and 0.95 (SE 0.02), respectively. The difference in AUC between the remaining CEUS studies and HR-MRI studies was not statistically significant (Z=0.16; P=0.43). The sensitivity analysis for HR-MRI yielded robust results, as the aggregated values remained consistent even after the one-by-one removal of individual studies. *Tables 4* and *5* present the findings of the sensitivity analyses conducted for the CEUS and HR-MRI studies.

Publication bias

Results of Deeks funnel plots showed no statistically significant publication bias in the CEUS (P=0.85) or HR-MRI studies (P=0.78) (Figure S1A,S1B).

Conflicts of interest, funding source, and role of funding source

None of the studies reported a conflict of interest with the funding source or with the role of the funding source.

Discussion

Principal findings

This meta-analysis examined 839 patients across 20 studies comprising 1,357 plaques in HR-MRI and 504 plaques in CEUS to compare the diagnostic ability of these two modalities in evaluating the vulnerability of carotid artery plaques defined by histology. The results demonstrated that both CEUS and HR-MRI provide acceptable diagnostic accuracy, with high AUC values (0.89 *vs.* 0.94). CEUS demonstrated comparable performance to HR-MRI in detecting unstable carotid atherosclerotic artery plaques. As it pertains to plaque components, CEUS appears to be superior in assessing IPN and morphological changes, while MRI is more suited for assessing IPH and LRNC.

To our knowledge, only one systematic review has compared CEUS and HR-MRI in terms of plaque vulnerability assessment (13). Our review is novel for the following reasons: First, although we used the same search strategy as that of Li *et al.*, we included twice as many articles (with the exception of two recent studies published in 2022–2023), allowing for a more thorough evaluation

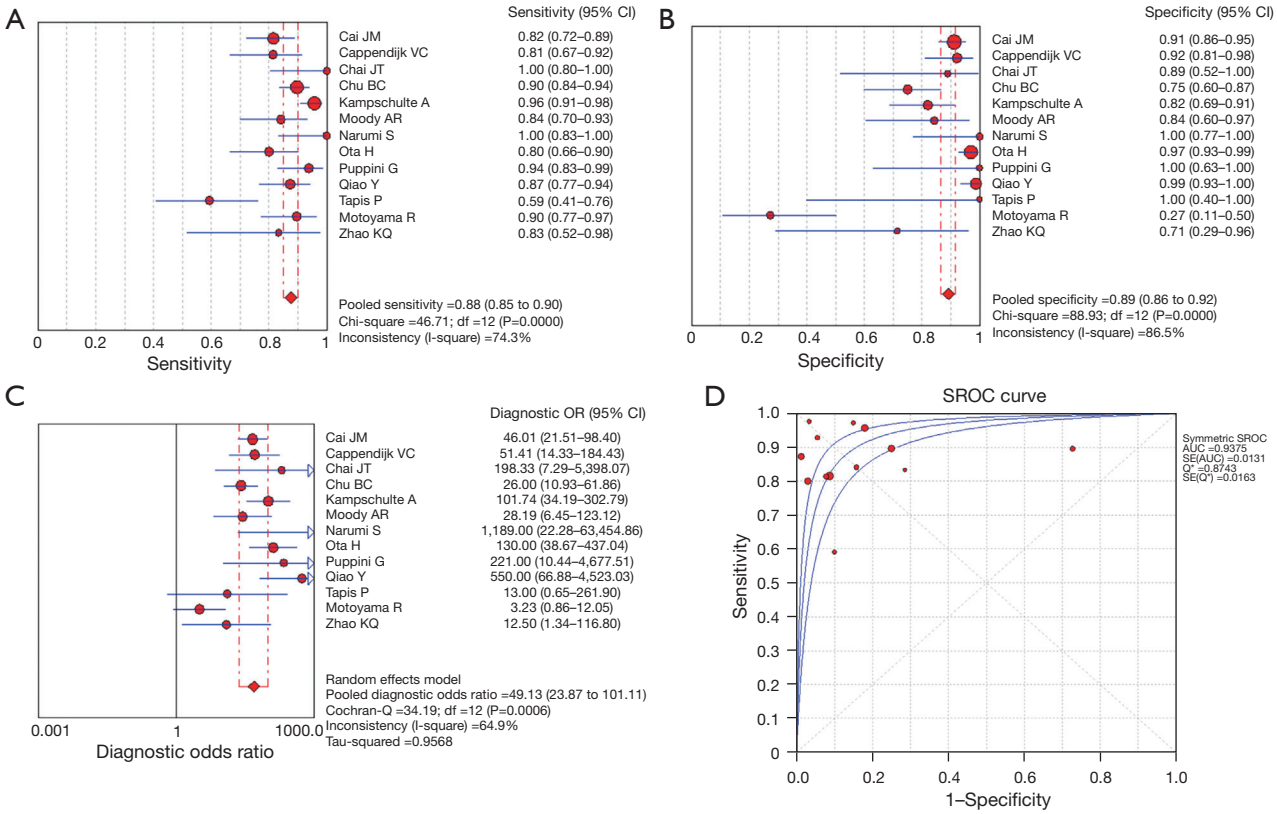

Figure 4 Forest plots of (A) sensitivity, (B) specificity, (C) diagnostic odds ratio, and (D) the summary receiver operator characteristic curve of the HR-MRI studies. In (D), the first and the third blue lines represent the 95% confidence interval of AUC, and the second blue line represents the regression line. CI, confidence interval; OR, odds ratio; SROC, summary receiver-operating characteristic; AUC, area under the curve; SE, standard error; HR-MRI, high-resolution magnetic resonance imaging.

of the diagnostic performance. Second, due to high and moderate heterogeneity among the CEUS and HR-MRI studies, respectively, we conducted subgroup analyses based on study design, plaque composition, MI, and JCR region (*Table 3*), which enabled us to determine the source of heterogeneity. Third, we summarized the value of the two imaging methods for identifying distinct plaque components using the pathological findings as a reference.

Diagnostic performance of CEUS

Our meta-analysis revealed that CEUS had a pooled sensitivity of 0.82 (95% CI: 0.78–0.87) and a specificity of 0.76 (95% CI: 0.68–0.83), which is higher than that reported by Li *et al.* (13) but lower than that reported by Huang *et al.* (12). In contrast to Huang *et al.*'s review (12), where CEUS was used for diagnosing IPN based on histological specimens or the clinical diagnosis of symptomatic plaques, our study focused on detecting vulnerable plaques using CEUS with histologic confirmation. The relevant evidence suggests that neovascularization is a prominent feature of vulnerable plaques (37), originating from the vasa vasorum (VV) network in the outer adventitia, which is simply structured and exhibits high permeability with increased VV density preceding intima thickening and endothelial dysfunction (38). The outer adventitia VV not only contributes to IPN but also serves as a pathway for inflammatory cells to infiltrate the plaque, directly exacerbating its vulnerability. Vascular endothelial growth factor (VEGF) is responsible for angiogenesis, vascular permeability, and endothelial maintenance (39). Both animal and human studies have reported a higher expression of VEGF-positive microvessels in vulnerable plaques compared to stable ones, with these markers showing a positive linear correlation with plaque enhancement on CEUS (19,40). In addition to IPN, plaques with complex

Table 3 Subgroup analysis of the CEUS and HR-MRI studies

Subgroup	CEUS			HR-MRI		
	Studies (n)	DOR (95% CI)	Heterogeneity, I^2 (%) (P)	Studies (n)	DOR (95% CI)	Heterogeneity, I^2 (%) (P)
Region						
Asia	5	41.43 (17.62–97.41)	0.0 (0.44)	6	54.44 (10.27–288.43)	79.8 (<0.001)
Europe	4	12.57 (0.73–215.56)	92.1 (<0.001)	7	53.72 (28.90–99.87)	29.0 (0.20)
Study design						
Prospective	5	15.16 (1.55–148.01)	89.9 (<0.001)	10	43.12 (19.12–97.25)	67.5 (0.001)
Retrospective	4	57.49 (10.28–321.62)	63.7 (0.04)	3	81.39 (12.30–538.53)	61.1 (0.08)
Sample size						
≥50	6	31.08 (3.18–303.68)	90.7 (<0.001)	8	45.74 (20.08–104.21)	74.8 (<0.001)
<50	3	19.29 (6.42–57.97)	0.0 (0.43)	5	68.08 (12.54–369.51)	36.0 (0.18)
Plaque composition						
IPN	6	24.85 (2.37–260.85)	89.4 (<0.001)	5	44.48 (10.86–182.24)	83.7 (0.0001)
Others	3	32.19 (12.98–83.49)	0.0 (0.44)	8	54.40 (28.21–104.90)	17.3 (0.29)
Mechanical index						
>0.2	4	34.10 (13.06–89.04)	0.0 (0.39)		–	–
≤0.2	5	18.33 (1.53–219.54)	91.3 (<0.001)		–	–
Strength field						
1.5 T		–	–	7	49.24 (28.77–84.26)	22.5 (0.26)
Others		–	–	6	41.73 (6.76–257.45)	80.8 (<0.001)
JCR region						
1	4	37.19 (0.83–1,668.75)	93.9 (<0.001)	8	54.16 (33.77–86.87)	16.3 (0.30)
≤2	5	21.57 (10.01–46.46)	0.0 (0.72)	5	41.07 (3.62–465.84)	82.2 (0.0002)

CEUS, contrast-enhanced ultrasound; HR-MRI, high-resolution magnetic resonance imaging; DOR, diagnostic odds ratio; CI, confidence interval; IPN, intraplaque neovascularization; JCR, Journal Citation Reports.

features such as prominent echolucency, ulceration, and intraplaque motion are closely associated with ischemic symptoms. Comped to conventional ultrasound (CUS), CEUS can provide clearer visualization of the plaque's boundaries. Three (17,18,20) out of the nine CEUS studies focused on identifying IPN within the plaque and also assessed plaque ulceration or morphological changes.

Sensitivity analysis revealed that the study conducted by D'Oria *et al.* (19) was the main factor contributing to the heterogeneity among the included CEUS studies. This discrepancy could be attributed to the variation in participant selection, as D'Oria *et al.* focused solely on patients with carotid stenosis over 70% who were asymptomatic, while the other studies included both symptomatic and asymptomatic individuals. Nevertheless, the authors demonstrated that there was no significant difference in plaque enhancement between histologically proven vulnerable plaque [American Heart Association (AHA) class VI] and stable plaque (AHA class IV/V). This finding does not diminish the significance of CEUS in detecting IPN.

Diagnostic performance of MRI

According to the available data, IPH is the most extensively documented independent risk factor for the recurrence of ipsilateral ischemia or transient ischemic attack in patients with carotid stenosis ≥50%, as indicated by carotid

Table 4 Sensitivity analysis of CEUS studies

Removed study	Sensitivity (95% CI)	Specificity (95% CI)	LR+ (95% CI)	LR– (95% CI)	DOR (95% CI)	AUC (SE)	Heterogeneity, I^2 (%) (P)
Fresilli D (17)	0.84 (0.79–0.88)	0.71 (0.62–0.79)	2.82 (1.48–5.37)	0.15 (0.05–0.45)	20.93 (4.19–104.53)	0.80 (0.10)	85.4 (<0.001)
Huang S (18)	0.85 (0.81–0.89)	0.76 (0.68–0.83)	3.34 (1.54–7.23)	0.14 (0.05–0.42)	27.39 (4.82–155.64)	0.89 (0.07)	87.3 (<0.001)
D'Oria (19)	0.92 (0.88–0.95)	0.80 (0.72–0.87)	4.00 (2.35–6.81)	0.12 (0.08–0.17)	41.49 (18.47–93.23)	0.95 (0.02)	25.4 (0.23)
Lyu Q (20)	0.85 (0.81–0.89)	0.73 (0.64–0.80)	2.92 (1.44–5.93)	0.14 (0.05–0.42)	24.03 (4.44–130.06)	0.86 (0.09)	86.4 (<0.001)
Di Leo (21)	0.85 (0.81–0.89)	0.78 (0.70–0.84)	3.80 (1.63–8.87)	0.13 (0.04–0.41)	32.65 (5.34–199.54)	0.89 (0.06)	87.6 (<0.001)
Iezzi R (22)	0.84 (0.80–0.88)	0.77 (0.69–0.84)	3.59 (1.55–8.33)	0.15 (0.05–0.43)	27.22 (4.73–156.75)	0.89 (0.07)	87.2 (<0.001)
Uchihara Y (23)	0.82 (0.78–0.87)	0.76 (0.68–0.83)	3.26 (1.55–6.88)	0.17 (0.07–0.47)	21.67 (4.30–109.26)	0.89 (0.06)	86.4 (<0.001)
Motoyama R (34)	0.84 (0.80–0.88)	0.78 (0.70–0.85)	3.76 (1.54–9.15)	0.14 (0.05–0.43)	29.87 (4.73–188.67)	0.90 (0.06)	87.4 (<0.001)
Zhao KQ (35)	0.85 (0.81–0.89)	0.76 (0.68–0.83)	3.36 (1.55–7.31)	0.15 (0.05–0.43)	25.97 (4.79–140.82)	0.89 (0.07)	87.3 (<0.001)

CEUS, contrast-enhanced ultrasound; CI, confidence interval; LR+, positive likelihood ratio; LR–, negative likelihood ratio; DOR, diagnostic odds ratio; AUC, area under the curve; SE, standard error.

Table 5 Sensitivity analysis of HR-MRI studies

Removed study	Sensitivity (95% CI)	Specificity (95% CI)	LR+ (95% CI)	LR– (95% CI)	DOR (95% CI)	AUC (SE)	Heterogeneity, I^2 (%) (P)
Chai JT (10)	0.87 (0.85–0.90)	0.89 (0.86–0.92)	7.60 (3.18–18.13)	017 (0.12–0.25)	46.73 (22.27–98.05)	0.93 (0.01)	67.0 (<0.001)
Hideki O (24)	0.88 (0.85–0.90)	0.87 (0.84–0.90)	6.56 (2.87–15.00)	0.16 (0.11–0.24)	44.07 (20.53–94.58)	0.93 (0.01)	64.2 (0.001)
Narumi S (25)	0.87 (0.85–0.90)	0.89 (0.86–0.91)	6.99 (3.02–16.14)	0.17 (0.12–0.25)	44.88 (21.94–91.83)	0.93 (0.01)	65.1 (<0.001)
Puppini G (26)	0.87 (0.84–0.89)	0.89 (0.86–0.91)	7.19 (3.09–16.70)	0.18 (0.12–0.26)	46.18 (22.02–96.83)	0.93 (0.01)	66.7 (<0.001)
Moody AR (27)	0.88 (0.85–0.90)	0.89 (0.87–0.92)	7.78 (3.20–18.89)	0.16 (0.11–0.24)	52.41 (23.91–114.89)	0.94 0.02)	67.5 (<0.001)
Cai JM (28)	0.88 (0.86–0.91)	0.88 (0.85–0.91)	7.42 (2.97–18.55)	0.16 (0.10–0.25)	51.12 (21.75–120.14)	0.94 (0.01)	67.8 (<0.001)
Kampschulte A (29)	0.86 (0.83–0.88)	0.90 (0.87–0.92)	7.90 (3.07–20.30)	0.19 (0.14–0.26)	45.39 (20.74–99.35)	0.92 (0.01)	65.2 (<0.001)
Chu B (30)	0.87 (0.84–0.90)	0.90 (0.88–0.93)	8.29 (3.09–22.24)	0.17 (0.11–0.25)	54.30 (23.95–123.10)	0.94 (0.01)	66.1 (<0.001)
Qiao Y (31)	0.88 (0.85–0.90)	0.88 (0.85–0.90)	6.37 (2.86–14.17)	0.17 (0.12–0.25)	41.21 (20.47–83.0)	0.93 (0.01)	61.3 (0.002)
Cappendijk VC (32)	0.88 (0.85–0.90)	0.89 (0.86–0.91)	7.28 (3.04–17.45)	0.16 (0.11–0.24)	49.59 (22.30–110.24)	0.94 (0.01)	67.8 (<0.001)
Tapis P (33)	0.89 (0.86–0.91)	0.89 (0.86–0.92)	7.59 (3.24–17.79)	0.15 (0.11–0.20)	52.21 (24.75–110.15)	0.94 (0.01)	67.2 (<0.001)
Motoyama R (34)	0.87 (0.85–0.90)	0.92 (0.89–0.94)	8.02 (5.00–12.86)	0.16 (0.11–0.23)	61.07 (34.56–107.9)	0.94 0.01)	38.9 (0.08)
Zhao KQ (35)	0.88 (0.85–0.90)	0.89 (0.87–0.92)	8.18 (3.39–19.75)	0.16 (0.11–0.24)	53.77 (25.37–113.98)	0.94 (0.01)	66.6 (<0.001)

HR-MRI, high-resolution magnetic resonance imaging; CI, confidence interval; LR+, positive likelihood ratio; LR–, negative likelihood ratio; DOR, diagnostic odds ratio; AUC, area under the curve; SE, standard error.

plaque on MRI (6,41). Zhou *et al.* (11) performed a meta-analysis to determine the pooled diagnostic accuracy of HR-MRI in detecting IPH and compared to our results, found a comparable sensitivity (0.87 *vs.* 0.88) but higher specificity (0.92 *vs.* 0.89). Our study aimed to incorporate all vulnerable plaque components that could be detected by HR-MRI. Within the MRI studies analyzed, seven focused on detecting IPH (24,25,29-32,34) and three on classifying LRNCs (10,26,33). The relationship between plaque composition and cardiovascular events remains a topic of ongoing debate. Longitudinal research over 4 years used serial MRI observed dramatic changes in plaque

characteristics, with an IPH and LRNC incidence of 18.5% and 39.6%, respectively (42). Although one study found no association between IPH and symptomatic status (36), it did report a slight correlation between IPH and adverse cardiovascular events. Conversely, LRNC content was found to be significantly higher in systematic plaques (10) and linked to a poor prognosis (43). Notably, a clear relationship exists between IPH, necrotic core expansion, and plaque vulnerability. Additionally, patients undergoing lipid-lowering therapy show increased lipid content in plaques with IPH and decreased content in those without IPH (44), indicating that IPH alone does not encompass all vulnerable or symptomatic plaques.

Implications for clinical practice

Although CEUS and HR-MRI evaluate distinct aspects of vulnerable plaque composition, their combined used can enhance the precision in symptomatic plaque diagnosis, outperforming magnetization-prepared rapid acquisition with gradient echo alone (AUC 0.79 *vs.* 0.58) (34). According to the Plaque–Reporting and Data System (45), which is based on gray-scale and color Doppler ultrasound, computed tomography angiography, and HR-MRI findings rather than CEUS findings, IPH, IPN, LRNC, and ulceration are key parameters of vulnerable plaques, although IPN has been incorporated as an ancillary feature (37). Pathologically, there is a close relationship between IPH, IPN, and LRNC. The presence of IPH without IPN is rare; nonetheless, extensive IPN can exist without IPH and is still related to plaque vulnerability (34). IPN plays a key role in plaque progression, as fragile neovessels are prone to bleeding. When driven by microenvironmental alternations or inflammatory factors, rupture of IPN leads to the emergence of IPH, with the latter resulting in enlargement of the LRNC and consequently a poor prognosis. In general, CEUS is performed with CUS and color Doppler ultrasound, both of which are cost-effective and convenient for follow-up, enabling the assessment of plaque status and luminal stenosis through gray-scale scoring and flow velocity measurements. Meanwhile, chronic IPH, characterized by hypointensity in all contrast weightings on MRI, can be mistaken for calcification, leading to FNs (30). Although CUS can easily identify calcification, pseudoenhancement, an artifact commonly seen in the far wall of the carotid artery, can mimic contrast enhancement on CEUS. Therefore, HR-MRI and CEUS can complement one another, each capable of detecting different plaque components with their own set of benefits and limitations. The most appropriate examination strategy for identifying susceptible plaques in clinical practice should be determined according to the patient's particular condition and the resources of the healthcare facility.

It is worth noting that the imaging characteristics of the plaques were contrasted with pathologic findings in all studies to confirm if these plaques are vulnerable; however, truly unstable plaques are associated with the occurrence of a clinical event (e.g., transient ischemic attack or stroke) (46), and current imaging assessments of plaque vulnerability only indicate morphological vulnerability. Therefore, follow-up of clinical outcomes is necessary to further determine the true clinical value of both modalities in the assessment of plaque instability. Furthermore, the development and model construction of artificial intelligence algorithms based on CEUS and MRI have shown great potential for application in plaque classification and segmentation (47). In the future, the innovation of artificial intelligence algorithms through the combination of these two modalities may have the potential to facilitate the identification of plaques morphologically and via microenvironmental changes.

Limitations

This study involved several limitations that should be addressed. First, the comparison of diagnostic performance between CEUS and HR-MRI in evaluating vulnerable carotid plaques was limited by the inclusion of only two paired studies in this review. Most CEUS studies focused on IPN detection and morphological changes, while many MRI studies focused on IPH and LRNCs. Therefore, future paired trials targeting the same plaque component may prove valuable for assessing and comparing the diagnostic efficacy of these two modalities. Second, CEUS lacks a uniform qualitative analysis and set of visual grading scale criteria. Data were extracted from a 2×2 table for analysis, and conducting subgroup analysis for various grade scales is challenging. Additionally, unstable plaques are more likely to be found in patients undergoing carotid endarterectomy for relevant symptomatic stenosis. It is worth noting that some studies categorized patients into symptomatic and asymptomatic groups, which hindered subgroup analyses based on symptomatic or asymptomatic cases. Furthermore, a limited number of studies prevented us from conducting a subgroup analysis of the variable scanning sequences in HR-MRI studies.

Conclusions

Both CEUS and HR-MRI are valuable noninvasive diagnostic methods for identifying pathologically proven vulnerable carotid artery plaques and have comparable diagnostic performance. CEUS is more capable of detecting IPN and ulceration, whereas HR-MRI is better suited to classifying IPH and LRNC. CEUS may serve as a potential alternative imaging tool to HR-MRI in assessing carotid plaque vulnerability under certain conditions. However, the published results, sample sizes, and studies incorporated were highly restrictive, and the interstudy heterogeneity was substantial. Further research on CEUS requires the implementation of standardized protocols for qualitative analysis to enhance the reliability and repeatability of results.

Acknowledgments

Funding: This work was supported by the National Natural Science Foundation of China (grant No. 82271995), the College Innovation Projects of Sichuan (grant No. S202310632255) and Cadre Health Research Project of Sichuan Province (No. 2021-1507).

Footnote

Reporting Checklist: The authors have completed the PRISMA-DTA reporting checklist. Available at https://qims.amegroups.com/article/view/10.21037/qims-24-540/rc

Conflicts of Interest: All authors have completed the ICMJE uniform disclosure form (available at https://qims.amegroups.com/article/view/10.21037/qims-24-540/coif). The authors have no conflicts of interest to declare.

Ethical Statement: The authors are accountable for all aspects of the work in ensuring that questions related to the accuracy or integrity of any part of the work are appropriately investigated and resolved.

References

1. Burkart KG, Brauer M, Aravkin AY, Godwin WW, Hay SI, He J, Iannucci VC, Larson SL, Lim SS, Liu J, Murray CJL, Zheng P, Zhou M, Stanaway JD. Estimating the cause-specific relative risks of non-optimal temperature on daily mortality: a two-part modelling approach applied to the Global Burden of Disease Study. Lancet 2021;398:685-97.
2. Global, regional, and national burden of stroke and its risk factors, 1990-2019: a systematic analysis for the Global Burden of Disease Study 2019. Lancet Neurol 2021;20:795-820.
3. Zhang R, Liu H, Pu L, Zhao T, Zhang S, Han K, Han L. Global Burden of Ischemic Stroke in Young Adults in 204 Countries and Territories. Neurology 2023;100:e422-34.
4. Piechocki M, Przewłocki T, Pieniążek P, Trystuła M, Podolec J, Kabłak-Ziembicka A. A Non-Coronary, Peripheral Arterial Atherosclerotic Disease (Carotid, Renal, Lower Limb) in Elderly Patients-A Review: Part I-Epidemiology, Risk Factors, and Atherosclerosis-Related Diversities in Elderly Patients. J Clin Med 2024.
5. Fabiani I, Palombo C, Caramella D, Nilsson J, De Caterina R. Imaging of the vulnerable carotid plaque: Role of imaging techniques and a research agenda. Neurology 2020;94:922-32.
6. Bos D, Arshi B, van den Bouwhuijsen QJA, Ikram MK, Selwaness M, Vernooij MW, Kavousi M, van der Lugt A. Atherosclerotic Carotid Plaque Composition and Incident Stroke and Coronary Events. J Am Coll Cardiol 2021;77:1426-35.
7. Cui L, Xing Y, Wang L, Chen H, Chen Y. Intraplaque neovascularisation is associated with ischaemic events after carotid artery stenting: an observational prospective study. Ther Adv Neurol Disord 2023;16:17562864221141133.
8. Hou C, Liu XY, Du Y, Cheng LG, Liu LP, Nie F, Zhang W, He W. Radiomics in Carotid Plaque: A Systematic Review and Radiomics Quality Score Assessment. Ultrasound Med Biol 2023;49:2437-45.
9. Hou C, Li S, Zhang L, Zhang W, He W. The differences between carotid web and carotid web with plaque: based on multimodal ultrasonic and clinical characteristics. Insights Imaging 2024;15:78.
10. Chai JT, Biasiolli L, Li L, Alkhalil M, Galassi F, Darby C, Halliday AW, Hands L, Magee T, Perkins J, Sideso

E, Handa A, Jezzard P, Robson MD, Choudhury RP. Quantification of Lipid-Rich Core in Carotid Atherosclerosis Using Magnetic Resonance T(2) Mapping: Relation to Clinical Presentation. JACC Cardiovasc Imaging 2017;10:747-56.
11. Zhou T, Jia S, Wang X, Wang B, Wang Z, Wu T, Li Y, Chen Y, Yang C, Li Q, Yang Z, Li M, Sun G. Diagnostic performance of MRI for detecting intraplaque hemorrhage in the carotid arteries: a meta-analysis. Eur Radiol 2019;29:5129-38.
12. Huang R, Abdelmoneim SS, Ball CA, Nhola LF, Farrell AM, Feinstein S, Mulvagh SL. Detection of Carotid Atherosclerotic Plaque Neovascularization Using Contrast Enhanced Ultrasound: A Systematic Review and Meta-Analysis of Diagnostic Accuracy Studies. J Am Soc Echocardiogr 2016;29:491-502.
13. Li Q, Cai M, Wang H, Chen L. Diagnostic Performance of Contrast-Enhanced Ultrasound and High-Resolution Magnetic Resonance Imaging for Carotid Atherosclerotic Plaques: A Systematic Review and Meta-Analysis. J Ultrasound Med 2023;42:739-49.
14. McInnes MDF, Moher D, Thombs BD, McGrath TA, Bossuyt PM; and the PRISMA-DTA Group; et al. Preferred Reporting Items for a Systematic Review and Meta-analysis of Diagnostic Test Accuracy Studies: The PRISMA-DTA Statement. JAMA 2018;319:388-96.
15. Whiting PF, Rutjes AW, Westwood ME, Mallett S, Deeks JJ, Reitsma JB, Leeflang MM, Sterne JA, Bossuyt PM; QUADAS-2 Group. QUADAS-2: a revised tool for the quality assessment of diagnostic accuracy studies. Ann Intern Med 2011;155:529-36.
16. Higgins JP, Thompson SG, Deeks JJ, Altman DG. Measuring inconsistency in meta-analyses. BMJ 2003;327:557-60.
17. Fresilli D, Di Leo N, Martinelli O, Di Marzo L, Pacini P, Dolcetti V, Del Gaudio G, Canni F, Ricci LI, De Vito C, Caiazzo C, Carletti R, Di Gioia C, Carbone I, Feinstein SB, Catalano C, Cantisani V. 3D-Arterial analysis software and CEUS in the assessment of severity and vulnerability of carotid atherosclerotic plaque: a comparison with CTA and histopathology. Radiol Med 2022;127:1254-69.
18. Huang S, Wu X, Zhang L, Wu J, He Y, Lai M, Xu J, Li Z. Assessment of Carotid Plaque Stability Using Contrast-Enhanced Ultrasound and Its Correlation With the Expression of CD147 and MMP-9 in the Plaque. Front Comput Neurosci 2021;15:778946.
19. D'Oria M, Chiarandini S, Pipitone MD, Fisicaro M, Calvagna C, Bussani R, Rotelli A, Ziani B. Contrast Enhanced Ultrasound (CEUS) Is Not Able to Identify Vulnerable Plaques in Asymptomatic Carotid Atherosclerotic Disease. Eur J Vasc Endovasc Surg 2018;56:632-42.
20. Lyu Q, Tian X, Ding Y, Yan Y, Huang Y, Zhou P, Hui P. Evaluation of Carotid Plaque Rupture and Neovascularization by Contrast-Enhanced Ultrasound Imaging: an Exploratory Study Based on Histopathology. Transl Stroke Res 2021;12:49-56.
21. Di Leo N, Venturini L, de Soccio V, Forte V, Lucchetti P, Cerone G, Alagna G, Caratozzolo M, Messineo D, Di Gioia C, Di Marzo L, Fresilli D, De Vito C, Pugliese G, Cantisani V, D'Ambrosio F. Multiparametric ultrasound evaluation with CEUS and shear wave elastography for carotid plaque risk stratification. J Ultrasound 2018;21:293-300.
22. Iezzi R, Petrone G, Ferrante A, Lauriola L, Vincenzoni C, la Torre MF, Snider F, Rindi G, Bonomo L. The role of contrast-enhanced ultrasound (CEUS) in visualizing atherosclerotic carotid plaque vulnerability: which injection protocol? Which scanning technique? Eur J Radiol 2015;84:865-71.
23. Uchihara Y, Saito K, Motoyama R, Ishibashi-Ueda H, Yamaguchi E, Hatakeyama K, Tanaka A, Kataoka H, Iihara K, Sugie K, Koga M, Toyoda K, Nagatsuka K, Ihara M. Neovascularization From the Carotid Artery Lumen Into the Carotid Plaque Confirmed by Contrast-Enhanced Ultrasound and Histology. Ultrasound Med Biol 2023;49:1798-803.
24. Ota H, Yarnykh VL, Ferguson MS, Underhill HR, Demarco JK, Zhu DC, Oikawa M, Dong L, Zhao X, Collar A, Hatsukami TS, Yuan C. Carotid intraplaque hemorrhage imaging at 3.0-T MR imaging: comparison of the diagnostic performance of three T1-weighted sequences. Radiology 2010;254:551-63.
25. Narumi S, Sasaki M, Natori T, Yamaguchi Oura M, Ogasawara K, Kobayashi M, Sato Y, Ogasawara Y, Hitomi J, Terayama Y. Carotid plaque characterization using 3D T1-weighted MR imaging with histopathologic validation: a comparison with 2D technique. AJNR Am J Neuroradiol 2015;36:751-6.
26. Puppini G, Furlan F, Cirota N, Veraldi G, Piubello Q, Montemezzi S, Gortenuti G. Characterisation of carotid atherosclerotic plaque: comparison between magnetic resonance imaging and histology. Radiol Med 2006;111:921-30.
27. Moody AR, Murphy RE, Morgan PS, Martel AL, Delay GS, Allder S, MacSweeney ST, Tennant WG, Gladman

J, Lowe J, Hunt BJ. Characterization of complicated carotid plaque with magnetic resonance direct thrombus imaging in patients with cerebral ischemia. Circulation 2003;107:3047-52.
28. Cai JM, Hatsukami TS, Ferguson MS, Small R, Polissar NL, Yuan C. Classification of human carotid atherosclerotic lesions with in vivo multicontrast magnetic resonance imaging. Circulation 2002;106:1368-73.
29. Kampschulte A, Ferguson MS, Kerwin WS, Polissar NL, Chu B, Saam T, Hatsukami TS, Yuan C. Differentiation of intraplaque versus juxtaluminal hemorrhage/thrombus in advanced human carotid atherosclerotic lesions by in vivo magnetic resonance imaging. Circulation 2004;110:3239-44.
30. Chu B, Kampschulte A, Ferguson MS, Kerwin WS, Yarnykh VL, O'Brien KD, Polissar NL, Hatsukami TS, Yuan C. Hemorrhage in the atherosclerotic carotid plaque: a high-resolution MRI study. Stroke 2004;35:1079-84.
31. Qiao Y, Etesami M, Malhotra S, Astor BC, Virmani R, Kolodgie FD, Trout HH 3rd, Wasserman BA. Identification of intraplaque hemorrhage on MR angiography images: a comparison of contrast-enhanced mask and time-of-flight techniques. AJNR Am J Neuroradiol 2011;32:454-9.
32. Cappendijk VC, Cleutjens KB, Heeneman S, Schurink GW, Welten RJ, Kessels AG, van Suylen RJ, Daemen MJ, van Engelshoven JM, Kooi ME. In vivo detection of hemorrhage in human atherosclerotic plaques with magnetic resonance imaging. J Magn Reson Imaging 2004;20:105-10.
33. Tapis P, El-Koussy M, Hewer E, Mono ML, Reinert M. Plaque vulnerability in patients with high- and moderate-grade carotid stenosis - comparison of plaque features on MRI with histopathological findings. Swiss Med Wkly 2020;150:w20174.
34. Motoyama R, Saito K, Tonomura S, Ishibashi-Ueda H, Yamagami H, Kataoka H, Morita Y, Uchihara Y, Iihara K, Takahashi JC, Sugie K, Toyoda K, Nagatsuka K. Utility of Complementary Magnetic Resonance Plaque Imaging and Contrast-Enhanced Ultrasound to Detect Carotid Vulnerable Plaques. J Am Heart Assoc 2019;8:e011302.
35. Zhao KQ, Xie X, Yin HF, Zhao JL, Cao ZJ, Yang Y, Jiang C, Zhu RR, Wu WW. Clinical cohort study of imaging evaluation and postoperative pathology of carotid vulnerable plaque. Zhonghua Yi Xue Za Zhi 2018;98:2424-8.
36. Di Napoli A, Cheng SF, Gregson J, Atkinson D, Markus JE, Richards T, Brown MM, Sokolska M, Jäger HR. Arterial Spin Labeling MRI in Carotid Stenosis: Arterial Transit Artifacts May Predict Symptoms. Radiology 2020;297:652-60.
37. Hou C, Li MX, He W. Carotid Plaque-RADS: A Novel Stroke Risk Classification System. JACC Cardiovasc Imaging 2024;17:226.
38. Mulligan-Kehoe MJ. The vasa vasorum in diseased and nondiseased arteries. Am J Physiol Heart Circ Physiol 2010;298:H295-305.
39. Zhu F, Yuan S, Li J, Mou Y, Hu Z, Wang X, Sun X, Ding J, Zheng Z. Cilengitide Inhibits Neovascularization in a Rabbit Abdominal Aortic Plaque Model by Impairing the VEGF Signaling. Biomed Res Int 2021;2021:5954757.
40. Wu Y, Li X, Wang Z, Zhang S, Feng Y, Sun L. Real-time Elastography and Contrast-Enhanced Ultrasound for Evaluating Adventitia in the Early Diagnosis of Vulnerable Plaques: an Exploratory Study Based on Histopathology. Transl Stroke Res 2024;15:545-55.
41. van Dam-Nolen DHK, Truijman MTB, van der Kolk AG, Liem MI, Schreuder FHBM, Boersma E, Daemen MJAP, Mess WH, van Oostenbrugge RJ, van der Steen AFW, Bos D, Koudstaal PJ, Nederkoorn PJ, Hendrikse J, van der Lugt A, Kooi ME; PARISK Study Group. Carotid Plaque Characteristics Predict Recurrent Ischemic Stroke and TIA: The PARISK (Plaque At RISK) Study. JACC Cardiovasc Imaging 2022;15:1715-26.
42. Pletsch-Borba L, Selwaness M, van der Lugt A, Hofman A, Franco OH, Vernooij MW. Change in Carotid Plaque Components: A 4-Year Follow-Up Study With Serial MR Imaging. JACC Cardiovasc Imaging 2018;11:184-92.
43. Sun J, Zhao XQ, Balu N, Neradilek MB, Isquith DA, Yamada K, Cantón G, Crouse JR 3rd, Anderson TJ, Huston J 3rd, O'Brien K, Hippe DS, Polissar NL, Yuan C, Hatsukami TS. Carotid Plaque Lipid Content and Fibrous Cap Status Predict Systemic CV Outcomes: The MRI Substudy in AIM-HIGH. JACC Cardiovasc Imaging 2017;10:241-9.
44. Zhao XQ, Sun J, Hippe DS, Isquith DA, Canton G, Yamada K, Balu N, Crouse JR 3rd, Anderson TJ, Huston J 3rd, O'Brien KD, Hatsukami TS, Yuan C; AIM-HIGH Carotid MRI Substudy Investigators. Magnetic Resonance Imaging of Intraplaque Hemorrhage and Plaque Lipid Content With Continued Lipid-Lowering Therapy: Results of a Magnetic Resonance Imaging Substudy in AIM-HIGH. Circ Cardiovasc Imaging 2022;15:e014229.
45. Saba L, Cau R, Murgia A, Nicolaides AN, Wintermark M, Castillo M, et al. Carotid Plaque-RADS: A Novel Stroke Risk Classification System. JACC Cardiovasc Imaging

2024;17:62-75.
46. Jiang C, Meng Q, Zhao K, Zhao H, Zheng Z, Wu W, Zhao X. Vulnerable carotid plaque characteristics on magnetic resonance vessel wall imaging: potential predictors for hemodynamic instability during carotid artery stenting. Quant Imaging Med Surg 2023;13:3441-50.
47. Han N, Ma Y, Li Y, Zheng Y, Wu C, Gan T, Li M, Ma L, Zhang J. Imaging and Hemodynamic Characteristics of Vulnerable Carotid Plaques and Artificial Intelligence Applications in Plaque Classification and Segmentation. Brain Sci 2023;13:143.

Cite this article as: Hou C, Xuan JQ, Zhao L, Li MX, He W, Liu H. Comparison of the diagnostic performance of contrast-enhanced ultrasound and high-resolution magnetic resonance imaging in the evaluation of histologically defined vulnerable carotid plaque: a systematic review and meta-analysis. Quant Imaging Med Surg 2024;14(8):5814-5830. doi: 10.21037/qims-24-540

